Title
Revisiting the π → π* transition of the nitrite ion at the air/water interface: A combined experimental and theoretical study

Authors
Mizuno, Hikaru
Oosterbaan, Katherine J
Menzl, Georg
et al.

Publication Date
2020-07-01

DOI
10.1016/j.cplett.2020.137516

Peer reviewed

Title: Revisiting the π→π* Transition of the Nitrite Ion at the Air/Water Interface: A Combined Experimental and Theoretical Study

Author Names & Affiliations: Hikaru Mizuno[a,b,#], Katherine J. Oosterbaan[a,b,#], Georg Menzl[b,#], Jacklin Smith[a], Anthony M. Rizzuto[a,b,1], Phillip L. Geissler[a,b,*], Martin Head-Gordon[a,b,*], and Richard J. Saykally[a,b,*]

[a] Department of Chemistry, University of California, Berkeley, California 94720, United States

[b] Chemical Sciences Division, Lawrence Berkeley National Laboratory, Berkeley, California 94720, United States

[#] These authors contributed equally

ORCIDs

Hikaru Mizuno: 0000-0002-0860-1404

Katherine J. Oosterbaan: 0000-0001-6630-2296

Georg Menzl: 0000-0001-9984-274X

Jacklin Smith: 0000-0001-6752-0834

Anthony M. Rizzuto: 0000-0002-1430-4414

Phillip L. Geissler: 0000-0003-0268-6547

Martin Head-Gordon: 0000-0002-4309-6669

Richard J. Saykally: 0000-0001-8942-3656

Corresponding Authors:

*E-mail: geissler@berkeley.edu, TEL: (510) 642-8716

*E-mail: mhg@cchem.berkeley.edu, TEL: (510) 642-5957

*E-mail: saykally@berkeley.edu, TEL: (510) 642-8269

*Corresponding authors at Department of Chemistry, University of California, Berkeley, California 94720, United States

Notes: The authors declare no competing financial interests.

---

[1] Present Address: Department of Chemistry, Elon University, Elon, North Carolina 27244, United States

ABSTRACT. Broadband deep ultraviolet electronic sum frequency generation spectroscopy allows measurement of electronic $|\chi^{(2)}|^2$-spectra at aqueous interfaces, providing considerable improvement over deep ultraviolet electronic second harmonic generation spectroscopy that yields error-prone, pointwise spectra. Reexamination of the $\pi \rightarrow \pi^*$ transition of nitrite at the air/water interface reveals that the interfacial $|\chi^{(2)}|^2$-spectrum is strikingly similar to the bulk absorption spectrum. Molecular dynamics simulations and SOS-CIS(D_0) electronic structure calculations provide no evidence for the previously reported contact ion pair-induced red-shift of the $\pi \rightarrow \pi^*$ transition at the air/water interface. Our results thus revise the previous description for nitrite interfacial adsorption as a contact ion pair.

KEYWORDS. Interface, water, ion pairing, solvation, electronic sum frequency generation spectroscopy, second harmonic generation spectroscopy, molecular dynamics, SOS-CIS(D_0).

The behavior of ions at and near aqueous interfaces is of central importance in many chemical systems, including electrochemistry [1], atmospheric chemistry [2], and biochemistry [3], but remains incompletely understood. Recent experimental and theoretical studies have unambiguously shown that ions adsorb to the air/water interface, with compelling evidence for enhanced surface concentrations of larger, more polarizable, weakly solvated anions [4–6]. However, while the mechanism of this selective ion adsorption to the air/water interface has been shown to correlate strongly with ionic radii and hydration properties, considerable debate remains, with conflicting interpretations of experimental data and theoretical models [5–9]. In order to more completely understand the nature of ions at aqueous interfaces, additional experimental probes are necessary. While several powerful "surface sensitive" spectroscopic techniques are widely used in this context, probe depths vary, ranging from the outermost few layers (*e.g.*, 2nd-order nonlinear spectroscopy) to greater than ca. 5 nm (*e.g.*, photoelectron spectroscopy) depending on experimental conditions. In molecular dynamics simulations, the choices of parameters, initial conditions, thermodynamic constraints, or simulation sizes can significantly affect the end results and subsequent interpretations.

To further advance our fundamental understanding of the mechanism of selective ion adsorption at the air/water interface, measuring and interpreting detailed electronic spectra of interfacial ions presents a compelling prospect. Toward that end, our group has recently developed femtosecond broadband deep ultraviolet electronic sum frequency generation (DUV-ESFG) spectroscopy [10,11] that produces a broad, continuous, interfacial electronic $|\chi^{(2)}|^2$-spectrum in a single measurement. Compared to time-consuming, error-prone *pointwise* measurements with resonant deep ultraviolet electronic second harmonic generation (DUV-ESHG) spectroscopy [4,5,12] that yields incomplete spectra, *broadband* DUV-ESFG spectroscopy allows a more

quantitative analysis of interfacial electronic $|\chi^{(2)}|^2$-spectra. Under the electric dipole approximation, SFG and SHG primarily sample the interfacial region (ca. 1 nm) where the inversion symmetry is inherently broken [13–15]. Herein, we employ broadband DUV-ESFG spectroscopy, MD simulations, and SOS-CIS(D_0) calculations to reexamine the $\pi \rightarrow \pi^*$ transition of nitrite (NO_2^-) at the air/water interface and compare the results with those from our previous DUV-ESHG study [16].

Nitrite is a relatively kosmotropic anion, similar in position to chloride and nitrate in the anion Hofmeister series: $F^- > Cl^- > NO_2^- > NO_3^- > Br^- > I^- > SCN^-$. Since nitrite is a major component of marine and terrestrial nitrogen cycles, nitrite photochemistry both directly and indirectly affects the global carbon cycle, marine habitats, and atmosphere, thus making this system of central interest and importance. In the atmosphere, photolysis of nitrite in seawater can form highly reactive hydroxyl (·OH) and nitric oxide (·NO) radicals, which can further react with volatile compounds [17–19]. As a weak kosmotrope, nitrite is not expected to exhibit strong surface concentration enhancement at the air/water interface. In 2009, Brown *et al*. used X-ray photoemission spectroscopy on a liquid jet to measure the depth profile of sodium nitrite and nitrate at the air/water interface and found both to be depleted relative to bulk concentrations; however, nitrite and nitrate were still *present* in the interfacial region (outermost ~2.5-3.0 nm, determined by photoelectron kinetic energy) [20].

The bulk UV-Vis spectrum of aqueous nitrite (Fig. 1a) exhibits an intense absorption band ($\varepsilon \approx 5800$ L mol^{-1} cm^{-1}) at 210 nm (5.90 eV) assigned to a $\pi \rightarrow \pi^*$ molecular transition [21–23]. Previous studies of the bulk spectrum have suggested that this band may engender transfer of an electron to the surrounding solvent, *i.e.*, is a charge-transfer-to-solvent (CTTS) band [24,25].

However, the observation of this band in crystalline sodium nitrite and the absence of CTTS-like solvent dependence in other solvents provide evidence against this CTTS assignment [21–23].

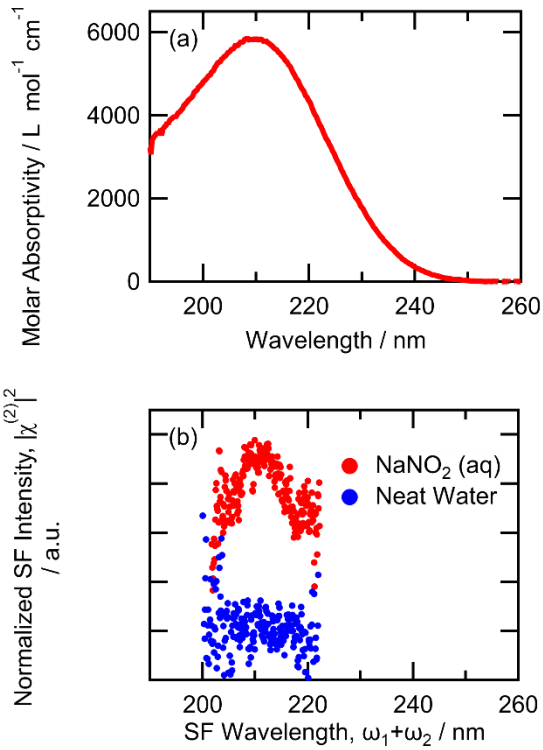

Figure 1. (a) Bulk UV-Vis absorption spectrum of aqueous sodium nitrite ([$NaNO_2$] = 180 µM). (b) Broadband interfacial $|\chi^{(2)}|^2$-spectrum measured by DUV-ESFG spectroscopy ($[NaNO_2]_{bulk}$ = 3.4 M). Spectra were measured at 293 K.

In 2012, Otten *et al.* reported pointwise DUV-ESHG spectra of sodium nitrite at the air/water interface and used a *bimolecular* Langmuir adsorption model to extract a surprisingly large and favorable Gibbs free energy of adsorption (ΔG_{ads} = -17.8 kJ mol^{-1}), suggesting adsorption as a Na^+-NO_2^- contact ion pair [16]. The ESHG spectra were measured at three wavelengths (λ_{SHG} = 200, 247, and 255 nm) showed strong resonance enhancement only at 247 nm, which led Otten and co-workers to report a significant red-shift (~0.75 eV) of the interfacial $\pi \rightarrow \pi^*$ transition relative to bulk that was attributed to contact ion pair formation and solvent effects [16].

In the interest of re-examining the nitrite $\pi \rightarrow \pi^*$ transition at the air/water interface, the $|\chi^{(2)}|^2$-spectrum of nitrite was measured with broadband DUV-ESFG spectroscopy between ~230-260 nm, but no significant resonance enhancement was observed [26]. The vibrational SFG spectrum of the nitrite solution showed sharp features at 2870 and 2933 cm^{-1}, corresponding to the -CH_3 symmetric stretch and its Fermi resonance, indicating the presence of hydrocarbons at the solution surface [26]. In solution, hydrocarbon impurities partition to the air/water interface and can contribute large non-resonant and/or resonant signals in SHG and SFG spectra [27]. The strong resonance enhancement observed exclusively at 247 nm in ESHG spectra by Otten *et al.* [16] may have resulted from aromatic structures and/or conjugated π-bond systems of hydrocarbon contaminants at the surface.

Herein, we report broadband DUV-ESFG spectrum of interfacial nitrite in the ~200-220 nm region. Ultrahigh purity sodium nitrite salt (Aldrich, 99.999% trace metals basis), baked overnight, was used to reduce effects of hydrocarbon contamination. All glassware was soaked in NOCHROMIX/sulfuric acid mixture overnight and washed with copious amounts of Milli-Q ultrapure water (18.2 MΩ.cm at 25 °C, TOC = 3 ppb), and solutions were prepared with Milli-Q ultrapure water immediately before measurements. The broadband DUV-ESFG spectroscopy

setup has been described in detail elsewhere [10,11]. Briefly, a 100-fs UV pulse (ω_1 = 266 nm) and a white light continuum pulse ($\omega_2 \approx$ 600-1400 nm) are temporally and spatially overlapped at the solution surface in reflection geometry, generating coherent sum frequency radiation ($\omega_1+\omega_2$) at the phase-matched angle [10,11]. The continuum pulse is generated by focusing the 800 nm output of a Ti-Sapphire amplifier into a quartz cuvette containing a continuous flow of water. This process gives rise to a positive temporal chirp of the broadband pulse [28]. Here, the longer wavelength portion (~800-1400 nm) of the broadband pulse is overlapped with the shorter, narrowband UV pulse. The raw ESFG spectrum is normalized by the SFG spectrum of a non-resonant sample (gallium arsenide, MTI Corporation) acquired under the same experimental conditions to correct for the spectral distortion and temporal chirp of the broadband pulse and the frequency-dependent efficiencies of the optics and CCD detector. The unnormalized spectra are shown in Figure S1 of the Supplementary Information. The white light continuum pulse and multiplex detection effects the measurement of a broadband electronic $|\chi^{(2)}|^2$-spectrum in a single measurement. Under the two-photon on-resonance, one-photon off-resonance condition employed here, the normalized ESFG intensity (I_{SFG}) can be expressed as

$$I_{SFG} \propto \left|\chi^{(2)}\right|^2 \propto \sum_n \frac{\left|\mu_{0n}(\alpha_{0n})_{2\mathrm{PA}}\right|^2}{(\omega_n - \omega_{\mathrm{SFG}})^2 + \Gamma_n^2}$$

where $\chi^{(2)}$ is the 2nd-order nonlinear susceptibility, μ_{0n} is the transition dipole matrix element and $(\alpha_{0n})_{2\mathrm{PA}}$ is the two-photon absorption polarizability tensor element connecting the ground state to excited state *n*, Γ_n is the linewidth of the transition, ω_n is the transition energy between the ground state and excited state *n*, and ω_{SFG} is the sum frequency of the input photons [29–31]. By plotting I_{SFG} vs. ω_{SFG}, the interfacial electronic $|\chi^{(2)}|^2$-spectrum is obtained. We note that the obtained $|\chi^{(2)}|^2$-spectrum is a power spectrum and that a more rigorous approach would be required to measure $\mathrm{Im}(\chi^{(2)})$ by heterodyne-detected or phase-sensitive ESFG spectroscopy; here, the non-resonant

contribution from the solvent (water) is assumed to be negligibly weak because no SFG signal is observed from the neat water surface (Figure S1).

The interfacial electronic $|\chi^{(2)}|^2$-spectrum (Fig. 1b), measured with broadband DUV-ESFG spectroscopy appears strikingly similar to the bulk absorption spectrum (Fig. 1a). Thus, we confirm the presence of nitrite at the air/water interface (outermost ~1 nm); however, we do not observe the previously reported drastic red-shift in the interfacial $\pi \rightarrow \pi^*$ transition, attributed to contact ion pairs and solvent effects [16]. In X-ray absorption spectra of bulk sodium nitrite solutions measured by the Saykally group, no appreciable ion pairing was observed [32]. We note, however, that the lower dielectric constant at the air/water interface [33,34] will increase the propensity for ion pair formation. Simulations by Venkateshwaran et al. have shown that ion pairing near the interface can be enthalpically and entropically favorable for oppositely charged ions, as it releases some hydrating waters to the bulk and reduces pinning of capillary waves [35]. At the concentrations used for the surface spectroscopy measurements discussed here, solvent separated, solvent shared, and contact ion pairs are likely to be present in the interfacial region. In addition, we note that an electric double layer can form in the interfacial region at moderate-to-high salt concentrations [36], which can induce ordering of water molecules and further alter the solvation environments at the interface. This induced ordering of water will increase the sampled "interfacial region" and thus may increase the probe depth of second order nonlinear spectroscopy techniques (e.g., SHS, SFG) at higher electrolyte concentrations [37].

To confirm the absence of a strong red-shift in the $\pi \rightarrow \pi^*$ transition induced by contact ion pair formation, MD simulations and electronic structure calculations were performed. Computing the $\pi \rightarrow \pi^*$ transition energy of nitrite in contact with sodium from electronic structure calculations requires equilibrium configurations of the non-electronic degrees of freedom, *i.e.*, the atomic

nuclei, as a starting point. Using empirical interaction potentials, we harvested such configurations from MD simulations of an ion pair in dilute bulk solution (numerical methods are described in the SI).

In order to identify contact ion pairs, we computed the potential of mean force as a function of the N–Na distance r, $w(r) = -k_B T \ln[P(r)/(4\pi r^2)]$, where k_B is Boltzmann's constant and $P(r)$ is the equilibrium probability distribution of the distance r between ions (Fig. 2).

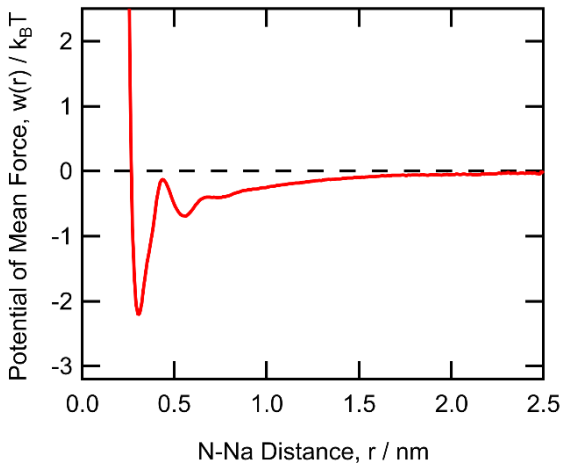

Figure 2. At low concentrations, the potential of mean force, $w(r)$, as a function of N–Na distance exhibits a minimum at ~0.3 nm that indicates the formation of contact ion pairs.

The potential of mean force encodes the effective Na^+-NO_2^- interaction as a function of distance when the ions' relative orientations and the solvent's degrees of freedom are canonically averaged over all configurations [38]. The minimum in $w(r)$ at $r \approx 0.3$ nm corresponds to contact ion pair configurations; based on these data, we selected configurations within $0.5\ k_B T$ of the minimum as input for the electronic structure calculations. To limit the computational cost of those calculations, only the water molecules in the first solvation shell of the ions, determined from the respective radial distribution functions, were taken into account.

SOS-CIS(D_0) calculations [39,40] were performed for the Na^+-NO_2^- contact ion pair and the isolated NO_2^- ion in vacuum and surrounded by its first solvent shell. This is the most extreme example of the potential effect of solvation and any difference here should be greater than what would be observed experimentally. SOS-CIS(D_0) was chosen because it has N^4 scaling and it was well-validated for nitrite against EOM-CCSD [41,42], which is accurate for single-electron valence excited states within 0.25 eV, while TDDFT [43–47] with various functionals was not. Calculations were performed in the def2-SVPD basis set [48,49].

In vacuum, the $\pi \rightarrow \pi^*$ transition of isolated nitrite occurred at 5.71 eV. The $\pi \rightarrow \pi^*$ transition of Na^+-NO_2^- contact pair showed some character at 5.37 eV and 5.80 eV in vacuum. However, when just two water molecules were added to a plane parallel with the contact ion pair, the energy of the transition stabilized to 5.69 eV, which we believe is closer to an accurate representation of the interface.

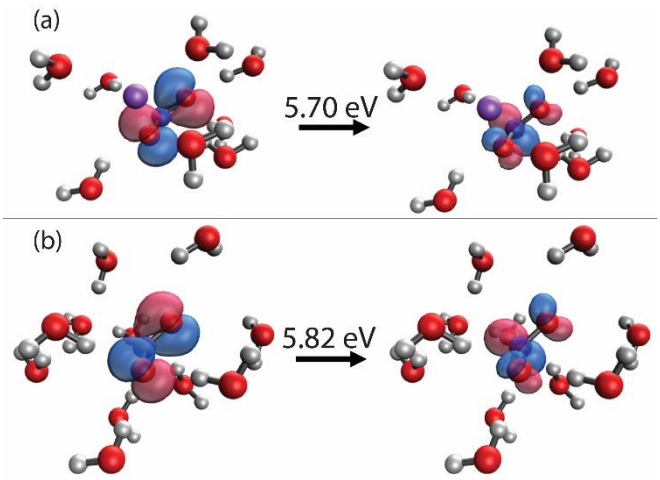

Figure 3. Representative snapshots and calculated $\pi \rightarrow \pi^*$ transition energies of (a) Na^+-NO_2^- contact ion pair in a solvent shell and (b) isolated NO_2^- ion in a solvent shell.

In order to get reproducible results, the geometry of NO_2^- in the solvent shell snapshots was slightly modified to be consistent with the vacuum geometry and looked at five randomly selected snapshots for the Na^+-NO_2^- contact pair and six for NO_2^-. While all NO_2^- snapshots had one distinct transition energy at which the $\pi \rightarrow \pi^*$ transition was found, the contact pair sometimes contained multiple transition energies with $\pi \rightarrow \pi^*$ character. To determine the average energy of the transition, we averaged all states at which $\pi \rightarrow \pi^*$ character was found. We found the $\pi \rightarrow \pi^*$ transition for the solvated Na^+-NO_2^- contact pair to be on average 5.70 eV (Fig 3a), and the $\pi \rightarrow \pi^*$ transition for solvated NO_2^- to be at 5.82 eV (Fig 3b). The differences between these values (0.12 eV), as well as the contrast between in vacuum and in solvation shell, are substantially smaller than the value reported by Otten *et al.*, which was ~0.75 eV [16].

We have employed broadband DUV-ESFG spectroscopy, MD simulations, and SOS-CIS(D_0) electronic structure calculations to re-examine the $\pi \rightarrow \pi^*$ transition of nitrite at the air/water interface. Our results, which reveal no significant shift in the $\pi \rightarrow \pi^*$ transition for the contact ion pair, revise our previously reported conclusions from pointwise DUV-ESHG spectra [16] that suggested a large red-shift at the surface and a bimolecular adsorption mechanism *via* contact ion pair formation. Although no evidence of a contact ion pair induced red-shift and strongly favorable bimolecular adsorption mechanism were found herein, our results do not rule out the presence of a distribution of local solvation environments at the interface, including solvent separated, solvent shared, contact ion pairs, and small ion clusters, under the experimental conditions discussed here.

ACKNOWLEDGMENTS

The work was supported by the U.S. Department of Energy, Office of Science, Basic Energy Sciences, under Contract No. DE-AC02-05CH11231, through the Chemical Sciences Division of the Lawrence Berkeley National Laboratory (LBNL). MD simulation results were obtained using the Savio computational cluster resource provided by the Berkeley Research Computing program at the University of California, Berkeley. The MD snapshot in the graphical abstract was generated using VMD [50].

REFERENCES

[1] S. Yoshimoto, K. Itaya, Adsorption and Assembly of Ions and Organic Molecules at Electrochemical Interfaces: Nanoscale Aspects, Annu. Rev. Anal. Chem. 6 (2013) 213–235. https://doi.org/10.1146/annurev-anchem-062012-092559.

[2] D.J. Tobias, A.C. Stern, M.D. Baer, Y. Levin, C.J. Mundy, Simulation and Theory of Ions at Atmospherically Relevant Aqueous Liquid-Air Interfaces, Annu. Rev. Phys. Chem. 64 (2013) 339–359. https://doi.org/10.1146/annurev-physchem-040412-110049.

[3] Y. Zhang, P.S. Cremer, Interactions between macromolecules and ions: the Hofmeister series, Curr. Opin. Chem. Biol. 10 (2006) 658–663. https://doi.org/10.1016/j.cbpa.2006.09.020.

[4] P.B. Petersen, R.J. Saykally, M. Mucha, P. Jungwirth, Enhanced concentration of polarizable anions at the liquid water surface: SHG spectroscopy and MD simulations of sodium thiocyanide, J. Phys. Chem. B. 109 (2005) 10915–10921. https://doi.org/10.1021/jp050864c.

[5] D.E. Otten, P.R. Shaffer, P.L. Geissler, R.J. Saykally, Elucidating the mechanism of

selective ion adsorption to the liquid water surface, Proc. Natl. Acad. Sci. 109 (2012) 701–705. https://doi.org/10.1073/pnas.1116169109.

[6] M. Mucha, T. Frigato, L.M. Levering, H.C. Allen, D.J. Tobias, L.X. Dang, P. Jungwirth, Unified picture of the surfaces of aqueous acid, base, and salt solutions, J. Phys. Chem. B. 109 (2005) 7617.

[7] E.A. Raymond, G.L. Richmond, Probing the molecular structure and bonding of the surface of aqueous salt solutions, J. Phys. Chem. B. 108 (2004) 5051–5059. https://doi.org/10.1021/jp037725k.

[8] S.J. Cox, P.L. Geissler, Interfacial ion solvation: Obtaining the thermodynamic limit from molecular simulations, J. Chem. Phys. 148 (2018). https://doi.org/10.1063/1.5020563.

[9] Y. Wang, S. Sinha, P.R. Desai, H. Jing, S. Das, Ion at air-water interface enhances capillary wave fluctuations: Energetics of ion adsorption, J. Am. Chem. Soc. 140 (2018) 12853–12861. https://doi.org/10.1021/jacs.8b06205.

[10] H. Mizuno, A.M. Rizzuto, R.J. Saykally, Charge-Transfer-to-Solvent Spectrum of Thiocyanate at the Air/Water Interface Measured by Broadband Deep Ultraviolet Electronic Sum Frequency Generation Spectroscopy, J. Phys. Chem. Lett. 9 (2018) 4753–4757. https://doi.org/10.1021/acs.jpclett.8b01966.

[11] A.M. Rizzuto, S. Irgen-Gioro, A. Eftekhari-Bafrooei, R.J. Saykally, Broadband Deep UV Spectra of Interfacial Aqueous Iodide, J. Phys. Chem. Lett. 7 (2016) 3882–3885. https://doi.org/10.1021/acs.jpclett.6b01931.

[12] P.B. Petersen, R.J. Saykally, Probing the interfacial structure of aqueous electrolytes with femtosecond second harmonic generation spectroscopy, J. Phys. Chem. B. 110 (2006) 14060–14073. http://pubs.acs.org/doi/abs/10.1021/jp0601825.

[13] V.P. Sokhan, D.J. Tildesley, The free surface of water: Molecular orientation, surface potential and nonlinear susceptibility, Mol. Phys. 92 (1997) 625–640. https://doi.org/10.1080/002689797169916.

[14] R.W. Boyd, Nonlinear Optics, Academic Press, 2008.

[15] Y.R. Shen, Fundamentals of Sum-Frequency Spectroscopy, Cambridge University Press, Cambridge, U.K., 2016.

[16] D.E. Otten, R.M. Onorato, R. Michaels, J. Goodknight, R.J. Saykally, Strong surface adsorption of aqueous sodium nitrite as an ion pair, Chem. Phys. Lett. 519–520 (2012) 45–48. https://doi.org/10.1016/j.cplett.2011.10.056.

[17] A. Treinin, E. Hayon, Absorption spectra and reaction kinetics of NO_2, N_2O_3, and N_2O_4 in aqueous solution, J. Am. Chem. Soc. 92 (1970) 5821–5828. https://doi.org/10.1021/ja00723a001.

[18] O.C. Zafiriou, M.B. True, Nitrite Photolysis in Seawater by Sunlight, Mar. Chem. 8 (1979) 9–32.

[19] D. Vione, V. Maurino, C. Minero, E. Pelizzetti, M.A.J. Harrison, R.-I. Olariu, C. Arsene, Photochemical reactions in the tropospheric aqueous phase and on particulate matter, Chem. Soc. Rev. 35 (2006) 441–453. https://doi.org/10.1039/b510796m.

[20] M.A. Brown, B. Winter, M. Faubel, J.C. Hemminger, Spatial Distribution of Nitrate and Nitrite Anions at the Liquid/Vapor Interface of Aqueous Solutions, J. Am. Chem. Soc. 131 (2009) 8354–8355. https://doi.org/10.1021/ja901791v.

[21] W.G. Trawick, W.H. Eberhardt, Electronic Transitions in the Nitrite Ion, J. Chem. Phys. 22 (1954) 1462. https://doi.org/10.1063/1.1740425.

[22] J.W. Sidman, Electronic and Vibrational States of the Nitrite Ion. I. Electronic States, J.

Am. Chem. Soc. 79 (1957) 2669–2675. https://doi.org/10.1021/ja01568a002.

[23] S.J. Strickler, M. Kasha, Solvent Effects on the Electronic Absorption Spectrum of Nitrite Ion, J. Am. Chem. Soc. 85 (1963) 2899–2901. https://doi.org/10.1021/ja00902a007.

[24] H.L. Friedman, On the ultraviolet absorption spectra of uninegative ions, J. Chem. Phys. 21 (1953) 319–322. https://doi.org/10.1063/1.1698879.

[25] G. Stein, A. Treinin, Electron-transfer spectra of anions in solution. Part 1.- Absorption spectra and ionic radii, Trans. Faraday Soc. 55 (1959) 1086–1090.

[26] A.M. Rizzuto, Investigation of the Surface Properties of Aqueous Solutions, University of California, Berkeley, 2016. https://escholarship.org/uc/item/78t6h56b.

[27] W. Hua, D. Verreault, E.M. Adams, Z. Huang, H.C. Allen, Impact of salt purity on interfacial water organization revealed by conventional and heterodyne-detected vibrational sum frequency generation spectroscopy, J. Phys. Chem. C. 117 (2013) 19577–19585. https://doi.org/10.1021/jp408146t.

[28] A. Brodeur, S.L. Chin, Ultrafast white-light continuum generation and self-focusing in transparent condensed media, J. Opt. Soc. Am. B. 16 (1999) 637. https://doi.org/10.1364/JOSAB.16.000637.

[29] A.J. Moad, G.J. Simpson, A Unified Treatment of Selection Rules and Symmetry Relations for Sum-Frequency and Second Harmonic Spectroscopies, J. Phys. Chem. B. 108 (2004) 3548–3562. https://doi.org/10.1021/jp035362i.

[30] C.-K. Lin, M. Hayashi, S.H. Lin, Theoretical Formulation and Simulation of Electronic Sum-Frequency Generation Spectroscopy, J. Phys. Chem. C. 117 (2013) 23797–23805. https://doi.org/10.1021/jp407881a.

[31] D. Bhattacharyya, H. Mizuno, A.M. Rizzuto, Y. Zhang, R.J. Saykally, S.E. Bradforth, New

Insights into the Charge-Transfer-to-Solvent Spectrum of Aqueous Iodide: Surface versus Bulk, J. Phys. Chem. Lett. 11 (2020) 1656–1661. https://doi.org/10.1021/acs.jpclett.9b03857.

[32] J.W. Smith, R.K. Lam, O. Shih, A.M. Rizzuto, D. Prendergast, R.J. Saykally, Properties of aqueous nitrate and nitrite from x-ray absorption spectroscopy, J. Chem. Phys. 143 (2015) 084503. https://doi.org/10.1063/1.4928867.

[33] L. Fumagalli, A. Esfandiar, R. Fabregas, S. Hu, P. Ares, A. Janardanan, Q. Yang, B. Radha, T. Taniguchi, K. Watanabe, G. Gomila, K.S. Novoselov, A.K. Geim, Anomalously low dielectric constant of confined water, Science. 360 (2018) 1339–1342. https://doi.org/10.1126/science.aat4191.

[34] S. Varghese, S.K. Kannam, J.S. Hansen, S. P. Sathian, Effect of Hydrogen Bonds on the Dielectric Properties of Interfacial Water, Langmuir. 35 (2019) 8159–8166. https://doi.org/10.1021/acs.langmuir.9b00543.

[35] V. Venkateshwaran, S. Vembanur, S. Garde, Water-mediated ion-ion interactions are enhanced at the water vapor-liquid interface, Proc. Natl. Acad. Sci. 111 (2014) 8729–8734. https://doi.org/10.1073/pnas.1403294111.

[36] T. Ishiyama, A. Morita, Intermolecular correlation effect in sum frequency generation spectroscopy of electrolyte aqueous solution, Chem. Phys. Lett. 431 (2006) 78–82. https://doi.org/10.1016/j.cplett.2006.09.024.

[37] S. Sun, J. Schaefer, E.H.G. Backus, M. Bonn, How surface-specific is 2nd-order non-linear spectroscopy?, J. Chem. Phys. 151 (2019). https://doi.org/10.1063/1.5129108.

[38] D. Chandler, Introduction to Modern Statistical Mechanics, 1st Ed., Oxford University Press, New York, 1987.

[39] Y.M. Rhee, D. Casanova, M. Head-Gordon, Performance of Quasi-Degenerate Scaled Opposite Spin Perturbation Corrections to Single Excitation Configuration Interaction for Excited State Structures and Excitation Energies with Application to the Stokes Shift of 9-Methyl-9,10-dihydro-9-silaphenanthrene, J. Phys. Chem. A. 113 (2009) 10564–10576. https://doi.org/10.1021/jp903659u.

[40] M. Head-Gordon, M. Oumi, D. Maurice, Quasidegenerate second-order perturbation corrections to single-excitation configuration interaction, Mol. Phys. 96 (1999) 593–602. https://doi.org/10.1080/00268979909482996.

[41] M. Schreiber, M.R. Silva-Junior, S.P.A. Sauer, W. Thiel, Benchmarks for electronically excited states: CASPT2, CC2, CCSD, and CC3, J. Chem. Phys. 128 (2008) 134110. https://doi.org/10.1063/1.2889385.

[42] D. Kánnár, P.G. Szalay, Benchmarking Coupled Cluster Methods on Valence Singlet Excited States, J. Chem. Theory Comput. 10 (2014) 3757–3765. https://doi.org/10.1021/ct500495n.

[43] E.K.U. Gross, J.F. Dobson, M. Petersilka, Density functional theory of time-dependent phenomena, in: Density Funct. Theory II, Springer-Verlag, Berlin/Heidelberg, 2005: pp. 81–172. https://doi.org/10.1007/BFb0016643.

[44] F. Furche, On the density matrix based approach to time-dependent density functional response theory, J. Chem. Phys. 114 (2001) 5982–5992. https://doi.org/10.1063/1.1353585.

[45] A. Görling, H.H. Heinze, S.P. Ruzankin, M. Staufer, N. Rösch, Density- and density-matrix-based coupled Kohn–Sham methods for dynamic polarizabilities and excitation energies of molecules, J. Chem. Phys. 110 (1999) 2785–2799. https://doi.org/10.1063/1.477922.

[46] R. Bauernschmitt, R. Ahlrichs, Treatment of electronic excitations within the adiabatic approximation of time dependent density functional theory, 1996.

[47] C. Jamorski, M.E. Casida, D.R. Salahub, Dynamic polarizabilities and excitation spectra from a molecular implementation of time-dependent density-functional response theory: N_2 as a case study, J. Chem. Phys. 104 (1996) 5134–5147. https://doi.org/10.1063/1.471140.

[48] D. Rappoport, F. Furche, Property-optimized Gaussian basis sets for molecular response calculations, J. Chem. Phys. 133 (2010) 134105. https://doi.org/10.1063/1.3484283.

[49] F. Weigend, R. Ahlrichs, Balanced basis sets of split valence, triple zeta valence and quadruple zeta valence quality for H to Rn: Design and assessment of accuracy, Phys. Chem. Chem. Phys. 7 (2005) 3297. https://doi.org/10.1039/b508541a.

[50] W. Humphrey, A. Dalke, K. Schulten, VMD: Visual molecular dynamics, J. Mol. Graph. 14 (1996) 33–38. https://doi.org/10.1016/0263-7855(96)00018-5.